

LETTER TO THE EDITOR

The bending of the star-forming main sequence traces the cold- to hot-accretion transition mass over $0 < z < 4$

Emanuele Daddi¹, Ivan Delvecchio², Paola Dimauro³, Benjamin Magnelli¹, Carlos Gomez-Guijarro¹, Rosemary Coogan¹, David Elbaz¹, Boris S. Kalita¹, Aurelien Le Bail¹, R. Michael Rich⁴, and Qing-hua Tan^{5,1}

¹ CEA, IRFU, DAp, AIM, Université Paris-Saclay, Université Paris Cité, Sorbonne Paris Cité, CNRS, 91191 Gif-sur-Yvette, France

² INAF-Osservatorio Astronomico di Brera, via Brera 28, 20121, Milano, Italy

³ INAF - Osservatorio Astronomico di Roma, Via di Frascati 33, 00078, Monte Porzio Catone, Italy

⁴ Department of Physics & Astronomy, University of California Los Angeles, 430 Portola Plaza, Los Angeles, CA 90095, USA

⁵ Purple Mountain Observatory, Chinese Academy of Sciences, 10 Yuanhua Road, Nanjing 210023, China

March 22, 2022

ABSTRACT

We analyse measurements of the evolving stellar mass (M_0) at which the bending of the star-forming main sequence (MS) occurs over $0 < z < 4$. We find $M_0 \approx 10^{10} M_\odot$ over $0 < z < 1$, then M_0 rises up to $\sim 10^{11} M_\odot$ at $z = 2$, and then stays flat or slowly increases towards higher redshifts. When converting M_0 values into hosting dark matter halo masses, we show that this behaviour is remarkably consistent with the evolving cold- to hot-accretion transition mass, as predicted by theory and defined by the redshift-independent M_{shock} at $z < 1.4$ and by the rising M_{stream} at $z \gtrsim 1.4$ (for which we propose a revision in agreement with latest simulations). We hence argue that the MS bending is primarily due to the lessening of cold-accretion causing a reduction in available cold gas in galaxies and supports predictions of gas feeding theory. In particular, the rapidly rising M_0 with redshift at $z > 1$ is confirming evidence for the cold-streams scenario. In this picture, a progressive fueling reduction rather than its sudden suppression in halos more massive than $M_{\text{shock}}/M_{\text{stream}}$ produces a nearly constant star-formation rate in galaxies with stellar masses larger than M_0 , and not their quenching, for which other physical processes are thus required. Compared to the knee M^* in the stellar mass function of galaxies, M_0 is significantly lower at $z < 1.5$, and higher at $z > 2$, suggesting that the imprint of gas deprivation on the distribution of galaxy masses happened at early times ($z > 1.5-2$). The typical mass at which galaxies inside the MS become bulge-dominated evolves differently from M_0 , consistent with the idea that bulge-formation is a distinct process from the phasing-out of cold-accretion.

Key words. Galaxies: evolution – Galaxies: formation – Galaxies: star formation – Galaxies: halos

1. Introduction

One of the key open issues in galaxy formation and evolution is understanding cold gas feeding of galaxies from the cosmic web sustaining their star-formation activity. Theory prescribes that cold gas accretes freely onto dark matter halos with mass $M_{\text{DM}} < M_{\text{shock}} \approx 10^{11.8} M_\odot$ at any redshift (Keres et al. 2005; Dekel & Birnboim 2006; DB06 hereafter), and crucially also onto more massive halos at high redshift where cold-streams, collimated flows of cold accreting gas, can penetrate efficiently for halos with $M_{\text{DM}} < M_{\text{stream}}(z)$ (DB06; Dekel et al. 2009). This $M_{\text{stream}}(z)$ boundary is predicted to lie at $\sim 10^{12.5} M_\odot$ at $z = 2$, growing to $\sim 10^{13.5} M_\odot$ at $z = 3$. Observational evidence for cold accretion and for the cold-stream scenario is still scarce.

Recently, Daddi et al. (2022; D22 hereafter) reported evidence for a progressive decrease in cold accretion for $M_{\text{DM}} > M_{\text{stream}}$ onto massive groups and clusters over $2 < z < 3.3$. They inferred that the fraction of baryonic accretion rate (BAR) remaining cold scales down like $(M_{\text{stream}}/M_{\text{DM}})^\alpha$, with slope $\alpha \sim 1$ and no apparent discontinuity up to two dex above M_{stream} . This result was primarily based on the extended Ly α emission luminosities, but slopes consistent with $\alpha \sim 1$ appeared to characterise also the star-formation rate (SFR) and bolometric active galactic nucleus (AGN) luminosities integrated over the massive halos. A modulation with slope $\alpha \sim 1$ implies that any quantity depending primarily upon cold accre-

tion, and thus rising (at fixed redshift) proportionally to M_{DM} for $M_{\text{DM}} < M_{\text{stream}}$ (or M_{shock}), would remain roughly constant at larger $M_{\text{DM}} > M_{\text{stream}}$ (see Eqs. 5 and 6 in D22, for Ly α).

It is intriguing that a similar mass dependence has been already recognised for the bending of the star-forming Main Sequence (MS), where SFR rises nearly linearly until a certain bending stellar mass (M_0), and stays constant at larger masses (e.g., Lee et al. 2015; Schreiber et al. 2015; Popesso et al. 2019). Accretion rates of cold gas should have a direct impact on the SFRs, hence it is quite natural that the distribution of SFRs in galaxies (and the MS) is an important observable where variations in accretion modes could be detected. The bending mass at $z \sim 0$ has been already noticed to be similar to the M_{shock} boundary (Popesso et al. 2019), once the average relation between stellar and halo mass is considered (Behroozi et al. 2013). Bending gets progressively weaker over $10^{10} M_\odot < M_* < 10^{11} M_\odot$ at $z > 1$ (Schreiber et al. 2015; Delvecchio et al. 2021), suggesting that M_0 increases strongly with redshift, qualitatively similar to the rise of the M_{stream} boundary. The analogies are so strong to warrant a quantitative examination.

In this letter we study the relation between M_0 and $M_{\text{shock}}/M_{\text{stream}}$ as a function of redshift, showing that they are essentially the same mass scale over $0 < z < 4$, and discuss the implications of this coincidence. We adopt concordance cosmology (0.3; 0.7; 70) and a Chabrier IMF.

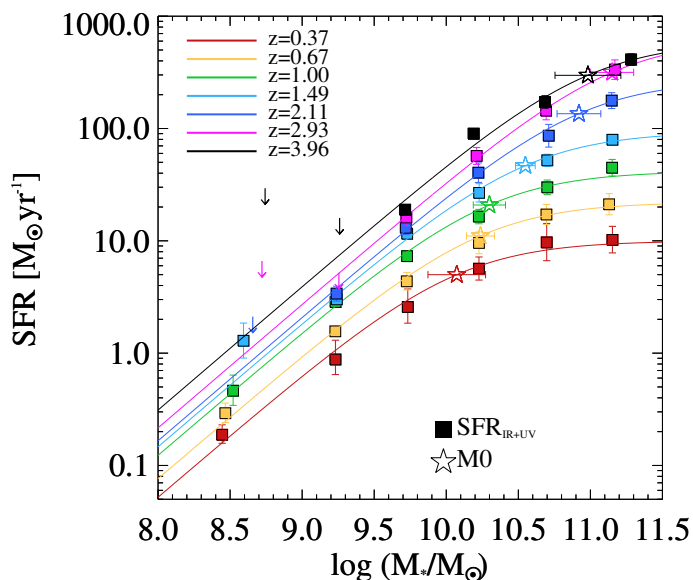


Fig. 1. The star-forming Main Sequence derived in redshift bins over $0.4 < z < 4.0$ (squares), adapted from Delvecchio et al. (2021). Solid lines show fits of Eq. 1 to the data. The bending stellar mass M_0 (see text for details) is shown as an empty star for each redshift bin (with its error). Notice how it rapidly increases from low- to high-redshifts.

2. Quantifying the redshift evolution of the bending of the star-forming Main Sequence

2.1. Bending formalism

The parametrisation for describing the MS (SFR vs. the stellar mass M_*) with its bending is adopted¹ from Lee et al. 2015 (L15 hereafter), that we rewrite as:

$$\frac{\text{SFR}}{\text{SFR}_0} = \frac{1}{1 + (M_0/M_*)^\gamma} \quad (1)$$

with M_0 being the *bending mass*, SFR_0 the SFR saturation limit for $M_* \gg M_0$, and γ the MS slope in the limit of $M_* \ll M_0$. Note that Eq. 1 implies $\text{SFR}(M_0)/\text{SFR}_0 = 0.5$ for any γ , hence the SFR only marginally further rises by $\times 2$ beyond M_0 .

There are strong analogies between Eq. 1 and the formalism from D22 (their Eqs. 1–4) describing quantities depending on cold accretion. While in D22 the equations relate to M_{DM} , and here to M_* , stellar and dark matter mass scales are tightly related on average (e.g., Behroozi et al. 2013). Also, the D22 formalism describes a stepwise behaviour across the $M_{\text{shock}}/M_{\text{stream}}$ boundaries (Eq. 3 in D22) while here we have a continuous function (Eq. 1), but the two can be shown to be fully consistent. We built a simple toy model with the expected behaviour from Eq. 3 in D22, adding appropriate noise in SFR as well as in the stellar-to-halo mass conversion. We find that M_0 as defined in Eq. 1 is an unbiased estimator of the stepwise boundary (i.e., $M_{\text{shock}}/M_{\text{stream}}$) in the presence of noise, to better than 0.02 dex.

The fact that Eq.1 converges to a constant SFR for $M_* \gg M_0$ is equivalent to using $\alpha \sim 1$ in D22 (and indeed the key result from D22 was to constrain $\alpha_{L_{\text{Ly}\alpha}} \sim 1$). The D22 formalism adopts in practice $\gamma = 1.15$ that is inherited by the predicted M_{DM} dependence of the BAR onto DM halos (Goerdt et al. 2009; Genel et al. 2008; Dekel et al. 2013) in the cold-stream or cold-accretion regimes. Indeed, as we will see in the following, the

¹ With the purely esthetical difference that we express parameters in linear instead of log space.

Table 1. Fitting of the star-forming MS with bending, in different redshift bins.

z	$\log M_0$ M_\odot	$\log \text{SFR}_0$ $M_\odot \text{ yr}^{-1}$	γ
Lee et al. 2015			
0.36	10.03 ± 0.14	0.80 ± 0.07	0.92 ± 0.06
0.55	9.82 ± 0.11	0.99 ± 0.05	1.13 ± 0.11
0.70	9.93 ± 0.11	1.23 ± 0.06	1.11 ± 0.09
0.85	9.96 ± 0.09	1.35 ± 0.05	1.28 ± 0.12
0.99	10.10 ± 0.10	1.53 ± 0.06	1.26 ± 0.11
1.19	10.31 ± 0.15	1.72 ± 0.08	1.07 ± 0.10
Delvecchio et al. 2021			
0.37	10.06 ± 0.18	1.02 ± 0.11	1.1
0.67	10.25 ± 0.09	1.34 ± 0.09	1.1
1.00	10.30 ± 0.11	1.62 ± 0.10	1.1
1.49	10.56 ± 0.07	1.98 ± 0.06	1.1
2.11	10.92 ± 0.14	2.43 ± 0.13	1.1
2.93	11.15 ± 0.16	2.81 ± 0.15	1.1
3.96	11.00 ± 0.21	2.79 ± 0.19	1.1

Notes: Lee et al. (2015) measurements were presented originally in their work, we have only scaled-up the uncertainties (see text). The parameters for Delvecchio et al. (2021) are derived in this work.

MS also implies $\gamma \sim 1.1$. This analogy between the MS slope and BAR (before bending happens) has already been discussed by Dekel et al. (2013). All of this suggests that to some extent M_0 might be equivalent to $M_{\text{shock}}/M_{\text{stream}}$, which we will demonstrate empirically in the following by deriving the redshift evolution of M_0 since $z = 4$ and comparing it to the $M_{\text{shock}}/M_{\text{stream}}$ masses over the same range.

2.2. Redshift evolution of bending

In order to be able to obtain reliable fits of the parameters from Eq. 1 it is required to have (1) a deep sample, reaching much fainter than M_0 (at any redshift, which is made easier by the implied redshift evolution of M_0 , as evident from the rest of this work). Also, (2) large statistics at the high M_* end are required, in order to derive SFR_0 , which demands large sky area; and (3) the use of consistent SFR indicators across the entire dynamic range. In this work we do not obtain new MS determinations, something already done in countless literature works (see Speagle et al. 2014 for a review). We adopt average SFR vs stellar mass (M_*) measurements from state of the art works (L15 and Delvecchio et al. 2021; D21 hereafter) spanning (when combined) $0 < z < 4$ with large statistics and reaching down to very low stellar masses which is essential for this analysis. These two works fulfill the mentioned requirements and are both based in the COSMOS field.

L15 measured the MS over 6 redshift bins with average $z = 0.36$ to 1.19 , using $\sim 62,000$ SF galaxies selected from Ilbert et al. (2013) using the NRK color method. SFRs are derived using a ladder approach, including UV, mid-IR and far-IR measurements. Their MS is obtained using a very finely binned grid to which they fitted Eq. 1, and report the 3 free parameters with formal uncertainties from the fit. From their Fig. 6 one can see that their M_0 values display a non-monotonous behaviour that is seemingly significant with respect to their reported error bars. E.g., M_0 significantly decreases from $z = 0.34$ to 0.51 , and jumps up again at $z = 0.70$ – 0.99 . We take this as evidence of underestimation of the uncertainties, e.g. due to degeneracies

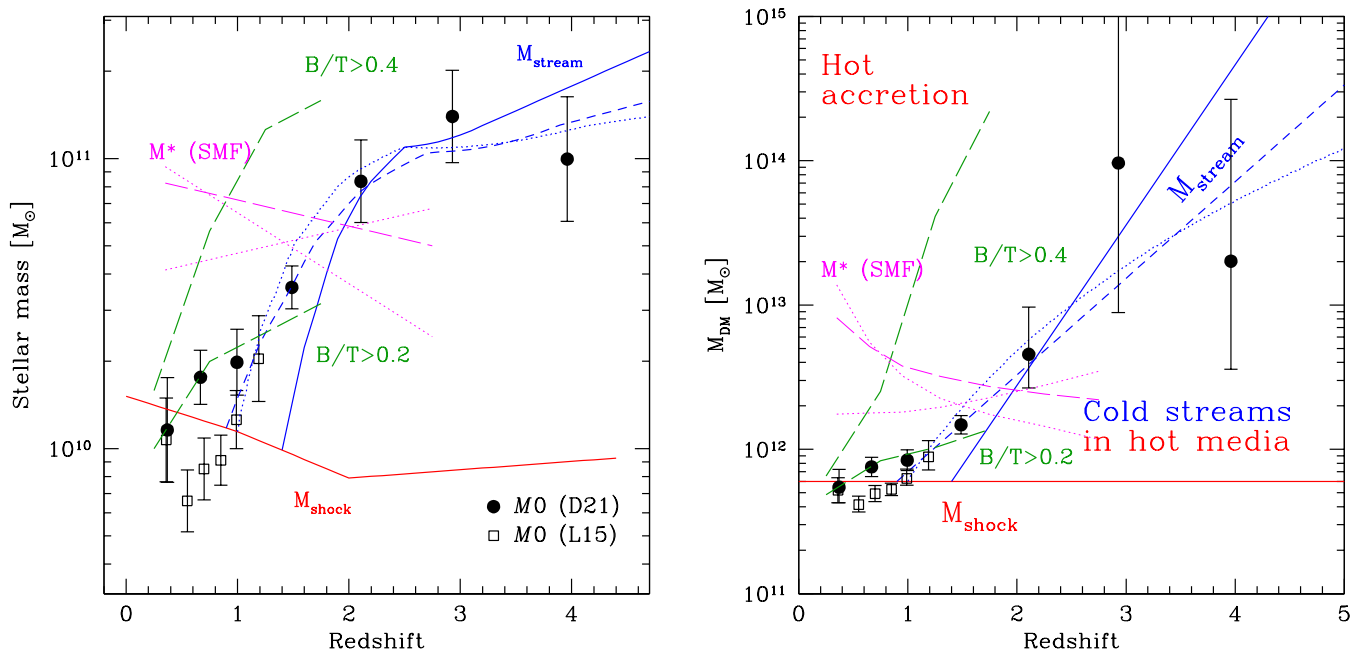


Fig. 2. Measurements of M_0 are shown in both panels from L15 (empty squares) and D21 (filled circles), together with the M_{shock} and M_{stream} boundaries (DB06, solid blue line; from our fit to the M_0 data as in Eq. 2, dashed blue line; based on Mandelker et al. 2020, dotted blue line). The M^* values for the stellar mass function (SMF) are from Ilbert et al. (2013; linear fit to their redshift trends; solid for the total, dotted for those of quiescent/SF galaxies that are decreasing/increasing with redshift, respectively). The green long-dashed lines show the masses at which the average bulge/total (B/T) ratio in MS galaxies rises above 0.2 and 0.4, derived from the measurements of Dimauro et al. (2022). Measurements and relations are converted from stellar to halo masses (and vice-versa) using the relations from Behroozi et al. (2013).

between parameters, and systematics. We find that scaling up the uncertainties by a factor of 3.4 is sufficient to remove the anomalous redshift fluctuations. A posteriori based on the minimum reduced χ^2 of the fit to all datasets, and also in comparison with the D21 dataset, we confirm that this scaling is indeed required. We apply this to all L15 parameter uncertainties. The L15 results with the proposed error rescaling are summarised in Table 1.

D21 measured the MS over 7 redshift bins with average $z = 0.37$ to 3.96 , using $\sim 400,000$ SF galaxies from Laigle et al. (2016), still selected using the NRJ color method (basically identical to the NRK but improving over it for the highest redshift range, implying full consistency with the L15 sample). For each redshift bin they defined large, 0.5 dex-wide stellar mass bins (except for the lowest and highest mass bins that are 1 dex wide) and measured the average SFR via stacking in multi-band far-IR datasets, including Herschel, Spitzer, SCUBA and AzTEC, and adding the contribution of un-observed UV. Because their binning is wide, to reduce the noise in the measurements we fixed the value of $\gamma = 1.1$, the average slope obtained by L15 using a much finer grid. Using free γ would not alter the conclusion of this work (and on average would still give a consistent $\gamma \sim 1.1$). We thus fitted Eq. 1 to the D21 data (Fig. 1) and estimated uncertainties in the best fitting parameters from Monte Carlo simulations. The measurements are in Table 1.

The M_0 measurements as a function of redshift are shown in Fig. 2-left. Derivations from L15 and D21 are in reasonably good agreement over $0.4 < z < 1.2$ where they define an average at the level of $M_0 \sim 10^{10} M_\odot$. The scatter between the two datasets allows us to gauge the underlying systematics. Mainly based on the D21 values, but also supported by the highest redshift point from L15 ($z = 1.2$), we see that M_0 rapidly increases above $z = 1$, to reach $M_0 \sim 10^{11} M_\odot$ at $z \gtrsim 2$.

2.3. Bending in halo mass space

We convert each M_0 measurement into the corresponding average M_{DM} value using the redshift-dependent relations from Behroozi et al. (2013; their Fig. 7-left). Such a relation is defined for central galaxies in each halo, or recently accreted satellites, but can be applied safely here because the vast majority of galaxies over the stellar mass ranges considered here are centrals (Popesso et al. 2019; McCracken et al. 2015). Fig. 2-right shows the evolution of M_0 when expressed in terms of average hosting DM halo mass. At $z < 1$ the typical M_0 corresponds to $\sim 4\text{--}8 \times 10^{11} M_\odot$, which is quite consistent with M_{shock} . Beyond $z \sim 1$ we see a rise until reaching $M_0 \sim 10^{13\text{--}14} M_\odot$ over $2 < z < 4$. This rise follows very closely the redshift dependence of M_{stream} and is quite consistent with its definition from DB06. The M_0 values expressed in terms of M_{DM} display large uncertainties at high masses/redshifts, due to the flattening of the M_*/M_{DM} relation at $M_* \gtrsim 10^{11} M_\odot$ (Behroozi et al. 2013), so that even relatively small uncertainties in M_* convert into large uncertainties in M_{DM} . To cope with this issue, in Fig. 2-left we show the M_{shock} and M_{stream} tracks converted from dark matter to stellar masses in the same way. This shows that at $z \simeq 2$ the M_0 measurements are in good agreement with M_{stream} expectations at $z \gtrsim 2$.

3. Refining the M_{stream} boundary

From Fig. 2 it is quite apparent that M_0 and $M_{\text{shock}}/M_{\text{stream}}$ are basically the same scale. However, there is a small discrepancy in the range $1 < z < 1.4$, due to the fact that M_0 rises up earlier than M_{stream} as originally predicted in DB06. As discussed at length in Dekel et al. (2009), the M_{stream} boundary was defined using ad-hoc assumptions, and its location would benefit from being refined by observations.

We use the evolving $M0$ data to find the best fitting $M_{\text{stream}}(z)$ relation, allowing its low-redshift intercept $z_{\text{stream,min}}$ and its slope to be free parameters (while keeping M_{shock} fixed at the DB06 value for $z < z_{\text{stream,min}}$). The best-fitting relation is:

$$\log M_{\text{stream}} \simeq \log M_{\text{shock}} + (0.67 \pm 0.15) \times (z - 0.9 \pm 0.1) \quad (2)$$

and it is shown in Fig. 2 as a dashed blue line. The best fit has $\chi_{\text{min}}^2 \sim 17.5$ with 11 d.o.f, which has a 10% probability to occur by chance (hence acceptable), showing that the error bars from our measurements are not severely underestimated. The two free parameters are somewhat correlated, in the sense that a higher $z_{\text{stream,min}}$ corresponds to a steeper relation. This relation has a lower $z_{\text{stream,min}}$ (0.9 vs 1.4) and a flatter slope (0.67 vs 1.11) with respect to the one from DB06 (see Eq. 2 in D22), which is a poorer representation of the $M0$ data ($\Delta\chi^2 \sim 37$).

Quite interestingly, if we were to adopt Eq. 2 as a definition of M_{stream} and repeat the analysis from D22 based on observations of 9 massive groups and clusters of galaxies at $2 < z < 3.3$, we find overall improvement in the significance of the D22 results. For example, the Ly α luminosities would provide $\alpha_{\text{Ly}\alpha} = 1.05 \pm 0.18$ (5.8 σ , vs 5.0 σ in D22) with a scatter of 0.28 dex (0.30 dex in D22). Similarly, the correlation with the integrated SFRs would reach 2.9 σ (vs 2.6 σ in D22), with a scatter of 0.43 dex (vs. 0.45 dex). There is thus encouraging and independent observational support that this revised relation might be a change in the right direction.

3.1. A flatter $M_{\text{stream}}(z)$ is consistent with state of the art simulations

Present-day numerical simulations and analytical work suggest that a crucial process in the cold-stream feeding of cold gas to halos/galaxies is the cooling of hot halo gas through the radiative turbulent mixing layer that forms at the boundary between the initially cold stream and the initially hot background circumgalactic medium (CGM; Mandelker et al. 2020a; Gronke & Oh 2020, Fielding et al 2020). The survival of the streams to hydrodynamical instabilities in the CGM until reaching the central galaxy requires that the cooling time in the mixing layer is significantly shorter than the disruption time, especially in highly turbulent environments such as the CGM (Gronke et al. 2022). This can equivalently be expressed as a requirement that the stream radius (R_s) is larger than the critical radius (R_{crit}) by a substantial factor (Gronke & Oh 2020; Kanjilal et al. 2021; Mandelker et al. 2020b). Defining $M_{\text{stream}}(z)$ as the locus where $R_s/R_{\text{crit}} = 20$ from the fiducial model in Mandelker et al. (2020b; see their Fig. 2 where this ratio is expressed as a function of M_{DM} and z) returns the dotted blue line shown in Fig. 2, which is in striking agreement with the $M0(z)$ data and our $M_{\text{stream}}(z)$ refinement (Eq. 2).

4. Discussion

The $M_{\text{shock}}/M_{\text{stream}}$ boundaries mark, as a function of redshift, the critical masses when cold-accretion is expected to subside and turn into hot-accretion, based on theory predictions. Fig. 2 shows that these mass scales are in good agreement with $M0(z)$, the mass at which the MS is bending. This is unlikely to happen by chance, given the complex redshift dependence. Also, there is a fairly reasonable physical explanation for this coincidence: when cold-accretion starts to be reduced, becoming an increasingly smaller fraction of the total baryonic accretion, less

fuel is available to galaxies to form stars, hence the SFRs of such massive galaxies deviate from the SFR- M_* trend defined by lower-mass galaxies, as advocated in gas-regulator models (e.g., Bouchè et al. 2010; Lilly et al. 2013). The lower gas fraction of galaxies above $M0$ is implied by the constancy of the star-formation efficiency versus mass across the $M_{\text{shock}}/M_{\text{stream}}$ boundary (e.g., Wang et al. 2022).

The main consequence of this coincidence between $M0$ and $M_{\text{shock}}/M_{\text{stream}}$ is thus that it appears inevitable to conclude that the bending of the MS, through cosmic time, is primarily due to the phasing out of cold accretion.

4.1. Cold accretion downfall does not produce quenching

Additionally, this allows us to go a step further, and notice that the physical consequence of the phasing-out of cold accretion is to produce a flat SFR- M_* relation, i.e. reaching constant SFR vs M_* as an asymptotic value (SFR0). This is equivalent to say, formally, that $\alpha \sim 1$ (see intro; D22). A constant SFR vs M_* , and at fairly high values, is still quite some relevant amount of activity, at odds with the often held conception that the shutting down of cold-accretion beyond the $M_{\text{shock}}/M_{\text{stream}}$ boundary induces *quenching*. We recall that quenched galaxies are defined as those with very low amounts of residual SFR, e.g. much lower than that of the MS (including its bending).

A slope $\alpha \sim 1$ implies, for example, that a halo with mass 10 \times above the boundary has a cold share of accretion of 10% of the total (Eq. 3 in D22). However, such a halo has a total accretion 10 \times larger than a halo at the boundary (Eq. 1 in D22). Ultimately the cold accretion rate remains constant at any halo mass above the boundary. Hence, even when cold accretion is strongly reduced in its effective fraction, in the range of masses we have been probing it is not reduced in absolute scale, preventing galaxies from becoming quenched. The obvious consequence of this is that there is not such a thing as *starvation* from cold gas accretion discontinuation, at least not in the typical ranges we have probed (up to 1 dex above $M0$ at $z < 1$ from this work, and up to 2 dex above M_{stream} from Ly α in D22); cold gas shut down is not sufficient for galaxies to starve to death. Moreover, this implies that physical processes other than the shutting down of cold-accretion are required to quench galaxies. This might well be mergers (e.g., Puglisi et al. 2021), AGN (e.g., Brusa et al. 2018) or instability driven (e.g., Kalita et al. 2022).

We exclude the possibility that cold accretion contraction in the hot-accretion regime induces lots of real quenching, but those galaxies escape from our sample due to selection effects. While this might be suspected, as by construction we study only SF galaxies, at the masses where $M0$ occurs the SF galaxies are much more numerous than quiescent ones, over the whole redshift range studied (Ilbert et al. 2013; their Fig.6).

4.2. Bending mass and the galaxy mass function of SF and quenched galaxies

In order to further gauge the significance of our results, it is worth comparing $M0$ to the characteristic ‘knee’ masses (M^*) in the galaxy stellar mass functions (SMFs), representing the mass at which the differential mass (and SFR) contribution peaks, and the mass above which galaxies become exponentially rarer. These are shown as magenta lines in Fig. 2 (including the total SMF, and SMFs for quiescent and SF galaxies). At $z < 1.5$, M^* in the SMF is always much more massive than the bending

mass, while at $z \gtrsim 2$ it is less massive. Hence, the cold-accretion to hot-accretion transition does not appear to relate in any simple way to M^* in the SMF of galaxies, and the definition of *typical* galaxy stellar masses. The M^* for SF galaxies though does decrease mildly with cosmic time, possibly influenced by the similar decrease of M_0 . As stars in quenched galaxies observed at $z \sim 0-1$ are very old, formed at early times, this supports the idea that the imprint of the downfall of gas accretion into the galaxies SMF also happened at early times ($z > 1.5-2$ – this is because the lessening of accretion will reduce the ability of galaxies to become much more massive). The M^* for quenched galaxies runs almost perpendicular to M_0 , increasing with cosmic time towards low-redshift, emphasising furthermore the poor causal connection between the build-up of quenched galaxies and cold-accretion presence or suppression thereof (at odds with what is discussed e.g. in Dekel et al. 2009). This is however consistent with the recent finding (Kalita et al. 2021) of an extremely old quenched galaxy in the cold gas rich RO-1001 environment (Daddi et al. 2021), and in general with the presence of quenched galaxies at $z \gtrsim 3-4$ (Valentino et al. 2020; D’Eugenio et al. 2020; 2021; Forrest et al. 2020).

4.3. Cold accretion downfall unrelated to the rise of bulges

It has been often remarked that galaxies more massive than the MS bending are increasingly hosting more massive bulges, to the extent that considering only the disk-like components and ascribing to them the SFR, one gets closer to a MS rising trend (Abramson et al. 2014; Schreiber et al. 2016; Mancini et al. 2019). It is worth reconsidering the matter here, in light of our systematic discussion of the evolution of M_0 . We use the results of Dimauro et al. (2018; 2019; 2022), that performed bulge-disk decomposition in $0 < z < 2$ galaxies in CANDELS, using a machine learning approach for identifying bulge+disk systems. Limiting the results only to color-selected SF galaxies as in this work, the stellar masses along the MS in which the average bulge/total (B/T) mass fraction in galaxies exceeds 0.2 and 0.4 can be derived (Fig. 2). The $B/T = 0.4$ threshold is generally much higher than M_0 , although getting closer to it towards $z = 0$. Clearly most of the mass in MS galaxies is contained in the disk, even well beyond M_0 , but the bulge fraction keeps increasing with time, probably due to the hierarchical assembly of the bulges, and possibly rejuvenation (e.g., Mancini et al. 2019). The $B/T = 0.2$ threshold is closer to M_0 over $0 < z < 2$. It still has though a distinct rise with redshift that is incompatible with the constant M_{shock} boundary. It appears thus that the growth of the bulges has little in common with the phasing out of cold accretion, as might be reasonably expected also because the high Sersic indices of bulges require more than simple removal of gas infall, but rather mergers. This conclusion is supported by the analysis in Freundlich et al. (2019) where no connection between gas scaling relations and morphology was detected. It is tantalising though that the $B/T = 0.4$ trend mimics quite closely the M_{stream} trend but shifted roughly by $\Delta z \sim 1$ to later times. This shift might track the required timescale between the formation of bulge stars and the assembly and quenching of those same bulges.

4.4. Evolution of bending as confirming evidence for the cold-streams scenario

The slope of the MS has been generally reported to be in the range of 0.5–0.9 (Speagle et al. 2014 for a review), shallower

than the dependence of BAR on the mass which reads 1.15 (e.g., Dekel et al. 2013). However the observational measurements are affected by the bending of the MS. The limiting slope at low masses would be a better comparison ground, and this is indeed typically > 1 , on average 1.1 in L15, remarkably close to the expected theory value. In addition, the redshift evolution rate in the normalisation of the MS has been estimated as going in the range $(1+z)^{2.8-3.5}$ (Speagle et al. 2014 for a review), much faster than the exponent of 2.25 expected from theory. Again, this is typically derived at $M_* \sim 5 \times 10^{10} M_\odot$, where all the values at $z < 2$ are strongly affected by bending, producing a spuriously fast evolution. When considering the MS bending, the overall behaviour of the MS seems to be in even much better agreement with theory than what was realised so far. The rise of M_0 aligned to that of M_{stream} is also further confirmation of the cold-stream theory, as discussed in this work.

To conclude, together with the results from D22, the evidence is accumulating that cold streams (or their modulation) have a measurable impact on galaxy formation and evolution. Systematically investigating the physical properties of galaxies above and below $M_0(z)$ will further enlighten the processes by which accretion from the cosmic web affects galaxies.

Acknowledgements. We thank Nir Mandelker for providing us with a current theory-based derivation of M_{stream} based on his recent work and for discussions.

References

- Abramson L. E., Kelson D. D., Dressler A., et al., 2014, ApJL, 785, L36.
 Behroozi P. S., Wechsler R. H., Conroy C., 2013, ApJ, 770, 57.
 Bouché N., Dekel A., Genzel R., et al., 2010, ApJ, 718, 1001.
 Brusa M., Cresci G., Daddi E., et al., 2018, A&A, 612, A29.
 Daddi E., Valentino F., Rich R. M., et al., 2021, A&A, 649, A78.
 Daddi E., Rich R. M., Valentino F., et al., 2022, ApJ, 926, L21 (D22).
 Dekel A., Birnboim Y., 2006, MNRAS, 368, 2 (DB06).
 Dekel A., et al., 2009, Natur, 457, 451
 Dekel A., Zolotov A., Tweed D., et al., 2013, MNRAS, 435, 999.
 Delvecchio I., Daddi E., Sargent M. T., et al., 2021, A&A, 647, A123 (D21).
 D’Eugenio C., Daddi E., Gobat R., et al., 2020, ApJL, 892, L2.
 D’Eugenio C., Daddi E., Gobat R., et al., 2021, A&A, 653, A32.
 Dimauro P., Huertas-Company M., Daddi E., et al., 2018, MNRAS, 478, 5410.
 Dimauro P., Huertas-Company M., Daddi E., et al., 2019, MNRAS, 489, 4135.
 Dimauro P., Daddi E., Shankar F., et al., 2022, MNRAS, submitted
 Fielding D. B., Tonnesen S., DeFelippis D., et al., 2020, ApJ, 903, 32.
 Forrest B., Marsan Z. C., Annunziatella M., et al., 2020, ApJ, 903, 47.
 Freundlich J., Combes F., Tacconi L. J., et al., 2019, A&A, 622, A105.
 Genel S., Genzel R., Bouché N., et al., 2008, ApJ, 688, 789.
 Goerdt, T., Dekel, A., Sternberg, A., et al., 2010 MNRAS, 407, 613-631.
 Gronke M., Oh S. P., 2020, MNRAS, 492, 1970.
 Gronke M., Oh S. P., Ji S., Norman C., 2022, MNRAS, 511, 859.
 Ilbert O., McCracken H. J., Le Fèvre O., et al., 2013, A&A, 556, A55.
 Kalita B. S., Daddi E., D’Eugenio C., et al., 2021, ApJL, 917, L17.
 Kalita B. S., Daddi E., Bournaud F., et al., 2022, A&A, submitted
 Kanjilal V., Dutta A., Sharma P., 2021, MNRAS, 501, 1143.
 Kereš, D., Katz, N., Weinberg, D. H., Davé, R. 2005, MNRAS, 363, 2.
 Laigle C., et al., 2016, ApJS, 224, 24.
 Lilly S. J., Carollo C. M., Pipino A., et al., 2013, ApJ, 772, 119.
 Lee N., Sanders D. B., Casey C. M., et al., 2015, ApJ, 801, 80 (L15).
 Mancini C., Daddi E., Juneau S., et al., 2019, MNRAS, 489, 1265.
 Mandelker N., Nagai D., Aung H., et al., 2020a, MNRAS, 494, 2641.
 Mandelker N., van den Bosch F. C., Nagai D., et al., 2020b, MNRAS, 498, 2415.
 McCracken H. J., Wolk M., Colombi S., et al., 2015, MNRAS, 449, 901.
 Popesso P., Concas A., Morselli L., et al., 2019, MNRAS, 483, 3213.
 Puglisi A., Daddi E., Brusa M., et al., 2021, NatAs, 5, 319.
 Rosdahl, J., & Blaizot, J. 2012, MNRAS 423, 344.
 Schreiber C., Pannella M., Elbaz D., et al., 2015, A&A, 575, A74.
 Schreiber C., Elbaz D., Pannella M., et al., 2016, A&A, 589, A35.
 Speagle J.S., Steinhardt C.L., Capak P.L., Silverman J.D., 2014, ApJS, 214, 15.
 Valentino F., Tanaka M., Davidzon I., et al., 2020, ApJ, 889, 93.
 Wang T.-M., Magnelli B., Schinnerer E., et al., 2022, arXiv:2201.12070